Inorganic Chemistry

Article

pubs.acs.org/IC

Contribution of Intramolecular NH···O Hydrogen Bonds to Magnesium−Carboxylate Bonds

Taka-aki Okamura* and Junko Nakagawa

Department of Macromolecular Science, Graduate School of Science, Osaka University, Toyonaka, Osaka 560-0043, Japan

Supporting Information

ABSTRACT: A series of magnesium carboxylate complexes containing intramolecular NH···O hydrogen bonds were synthesized. Their molecular structures were determined by X-ray analysis. A direct NH···O hydrogen bond to the coordinated oxygen atom elongated the Mg−O bond, while a hydrogen bond to the carbonyl group shortened the Mg−O bond. Double NH···O hydrogen bonds significantly lowered the basicity of the carboxylate anion and prevented coordination to the Mg ion in a *trans* configuration; however, a *cis*-dicarboxylate complex was successfully obtained. Strong coordination of water to the Mg^{2+} ion stabilizes the weak Mg−carboxylate bond at the *trans* position. In contrast, a weak Mg−carboxylate bond strengthens the Mg−O(water) bond, probably increasing the acidity. Based on the experimental results and theoretical calculations, a new switching mechanism is proposed. In the proposed mechanism, the acidity of the coordinated water on magnesium is controlled during catalytic hydrolysis in endonuclease.

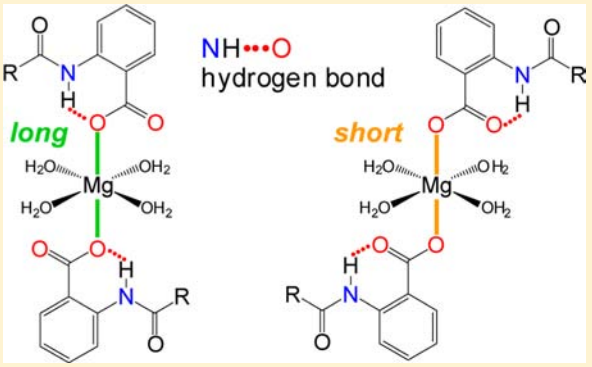

INTRODUCTION

Magnesium is widely distributed in seawater and soil and is a biologically essential element, playing very important roles in a wide range of enzymes in most living organisms. The major families of enzymes that use magnesium include kinase, ligase, and phosphatase. They are related to the phosphorylated compounds used in energy metabolism or storage of genetic information.[1] These are the key enzymes in the life cycles of cells and viruses deeply associated with serious diseases and repair of damaged DNA; e.g., a human immunodeficiency virus type I (HIV-1) integrase,[2] an avian influenza polymerase (PA_N),[3] DNA mismatch repair protein (MutS),[4] type II restriction endonuclease *Eco*RV,[5] and related enzymes.[6] These enzymes are activated by the addition of the Mg ion or a similar divalent metal ion (Mn^{2+}), depending on the concentration.[7] The coordination environment of biological magnesium complexes in enzymes has been described as a normal octahedral geometry with six-coordination around the Mg site, although some exceptions also exist.[8] The rigid coordination geometry is probably caused by the limited hybridization of s and p orbitals without the d orbital. A schematic drawing of the active site of endonuclease *Eco*RV[5] is shown in Figure 1. In the hydrolysis of the phosphodiester group, a water molecule or deprotonated hydroxide anion should attack the ester. The catalytic chemistry of magnesium-dependent enzymes has been described in the reviews.[9,10] The Mg ion acts as a Lewis acid to activate the bound substrate or water molecule and/or stabilizes the active species. The Mg ion affects the substrate directly (inner-sphere) or via water of hydration (outer sphere). Ionic or labile Mg−O bond shows

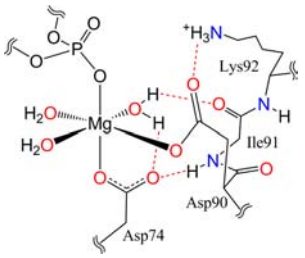

Figure 1. Schematic drawing of the active site of endonuclease *Eco*RV−substrate complex with the Mg^{2+} ion (PDB ID: 1RVB).[5]

different chemistry from the fourth-row elements, especially inert complexes. Hydrated chromium(III) effectively lowers the pK_a of the bound water to give Cr−OH^- species; however, the concentration of Mg−OH^- species is low, which unlikely acts as a nucleophile by inner-sphere pathway.[11] Obviously, the intramolecular direct attack to the neighboring phosphodiester is geometrically unfavorable and, therefore, improbable. It is reasonable that the Mg−OH^- species is readily protonated by outer-sphere water to give free OH^-.

Although the Mg ion is necessary to fix the substrate for site-specific cleavage, deprotonation of a water molecule bound to the Mg ion is one of the most plausible activation mechanisms described for the related zinc enzymes.[12,13] In the outer-sphere mechanism, the magnesium-bound OH^- generates a free hydroxide nucleophile by the deprotonation of outer-sphere

Received: March 20, 2013
Published: September 11, 2013

water.[10] Deprotonation of a water molecule on a Mg ion has been described in detail by Glusker et al. The theoretical calculations revealed that the presence of a Mg ion facilitates the ionization of water; however, the intramolecular OH···O hydrogen bond between water and carboxylate ligand does not appreciably affect the pK_a value.[14] Ionization of water is required to produce a nucleophile (OH^-). Increasing the acidity of water results in a weak conjugate base, according to the fundamental acid−base chemistry; however, a strong base is required for an effective nucleophilic attack. Assumption of a switching mechanism solves the contradiction, or coexistence, of a strong acid and base. Warshel et al. have proposed the external OH^- mechanism stabilized by Mg^{2+} ion based on theoretical calculations, thereby eliminating the dilemma mentioned above.[15] Indeed, pH dependency of Mg^{2+}-promoted reaction in aqueous media suggests the importance of free OH^- under pH-controlled conditions.[16] The question remains: How is pH or the reactivity of the enzyme controlled in natural systems? Moreover, theoretical interpretations of the experimental data for the related reactions are sometimes difficult or complicated.[17,18] If such a switching mechanism exists, which has never been proposed to our knowledge, the experimental observation could be more reasonably interpreted. In this Article, we explore the possibility of the regulation by hydrogen bonds in the magnesium−carboxylate coordination chemistry. In Figure 1, the NH···O hydrogen bond is found, along with the OH···O hydrogen bond, which is the most favorable candidate for the principal role in the switching mechanism.

Systematic investigations of NH···X (X = O, S, Se) hydrogen bonds to the coordinated X to metal ion (M) have revealed significant stabilization of the M−X bond.[19] At first, the effect of NH···S hydrogen bond to the covalent M−S (thiolate) bond was described.[20,21] This bond was seen in iron−sulfur proteins by crystallographic studies.[22] The hydrogen bond affects the covalent dπ−pπ interaction between the M (dπ) and S (pπ) atoms. Moreover, recent works on dioxomolybdenum(VI) complexes clearly indicated that the NH···S hydrogen bond stabilized a detached Mo═O bond via *trans* influence.[23−25] The study was extended to the more-covalent M−Se (selenolate)[26] and more-ionic M−O (carboxylate,[27] phosphate[28]) bonds. Interestingly, an NH···O hydrogen bond stabilized a Ca−O (carboxylate, phosphate) bond, which was believed to be ionic, by significant contribution of dπ−pπ interaction. This has been established both experimentally and theoretically, even though the d-orbital of the Ca^{2+} ion is formally vacant.[19,28] In the case of magnesium carboxylate, the d-orbital has an energy level that is too high to be used, making it unnecessary to consider the dπ−pπ interaction.

In this Article, we describe the synthesis of magnesium carboxylate complexes containing intramolecular NH···O hydrogen bonds and the contribution of hydrogen bonds to Mg−O bonds by X-ray analysis and theoretical calculations. An intraligand OH···O hydrogen bond in magnesium salicylate has already been reported.[29] Two types of ligands, with single and double intraligand NH···O hydrogen bonds, 2-$RCONHC_6H_4COOH$ (R = CH_3 (**L1**), CF_3 (**L2**)) and 2,6-$(RCONH)_2C_6H_3COOH$ (R = CH_3 (**L3**), CF_3 (**L4**), *t*-Bu (**L5**), *n*-Bu (**L6**)), were used; the deprotonated forms are shown in Chart 1. Fortunately, a rare mononuclear carboxylate complex in a *cis*-configuration was obtained by using **L6**.

Chart 1. Carboxylate Ligands Containing NH···O Hydrogen Bonds

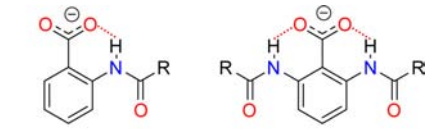

R = CH_3 (**L1**), CF_3 (**L2**) R = CH_3 (**L3**), CF_3 (**L4**), *t*-Bu (**L5**), *n*-Bu (**L6**)

EXPERIMENTAL SECTION

Materials. 2-$CH_3CONHC_6H_4COOH$ (**L1**) was obtained from Aldrich, and purified by recrystallization. 2,6-$(RCONH)_2C_6H_3COOH$ (R = CH_3 (**L3**), *t*-Bu (**L5**)) was prepared by the literature procedure.[30,31]

*2-$CF_3CONHC_6H_4COOH$ (**L2**).* To a tetrahydrofuran (THF) solution (10 mL) of 2-aminobenzoic acid (1.87 g, 16.6 mmol) was added trifluoroacetic anhydride (2.4 mL, 17.3 mmol) at 0 °C. After stirring overnight at room temperature, the solution was concentrated under reduced pressure to give a white powder. The residue was dissolved in ethyl acetate, washed with saturated NaCl aqueous solution, and dried over Na_2SO_4. After evaporation, the residual powder was recrystallized from diethyl ether/*n*-hexane to give colorless plates. Yield: 1.60 g (41.4%). ^{1}H NMR ($CDCl_3$): δ12.2 (1H, s), 8.67 (1H, d), 8.15 (1H, d), 7.65 (1H, t). 7.24 (1H, t). ESI-MS (methanol solution, negative mode): *m*/*z* 232.0 ($M-H^+$, calcd. 232.0), 487.1 ($2M-2H^++Na^+$, calcd. 487.0), 736.0 ($3M-2H^++K^+$, calcd. 736.0), 990.9 ($4M-3H^++Na^++K^+$, calcd. 991.0). Anal. Calcd for $C_9H_6F_3NO_3$: C, 46.36; H, 2.59; N, 6.01. Found: C, 46.00; H, 2.55; N, 6.21.

*2,6-$(CF_3CONH)_2C_6H_3COOH$ (**L4**).* This compound was synthesized by a similar method described in the report.[30] To a solution of 2,6-diaminotoluene (3.3 g, 27 mmol) in THF (40 mL) was added dropwise trifluoroacetic anhydride (10 mL, 70 mmol) cooling in an ice bath. After stirring overnight, volatile materials were removed under reduced pressure. Water was added to the resulting residue. The solid was filtered off, washed with a 2% HCl aqueous solution, water, 4% $NaHCO_3$ aqueous solution, and water, successively. The crude product was recrystallized from ethyl acetate. The product was collected with filtration, washed with diethyl ether, and dried over P_2O_5 in vacuo to give 2,6-$(CF_3CONH)_2C_6H_3CH_3$ in 90% yield. This compound (7.0 g, 22 mmol), $MgSO_4$ (2.7 g, 22 mmol), and $KMnO_4$ (7.0 g, 44 mmol) were suspended in water (300 mL). The mixture was stirred at 60 °C for 3 h and at room temperature overnight. Insoluble materials were filtered out. The filtrate was acidified by concentrated HCl to afford white solid, which was collected with filtration, washed with water, and dried over P_2O_5 under reduced pressure. Yield: 0.19 g (2.5%). ^{1}H NMR ($CDCl_3$): δ11.38 (2H, s), 8.45(2H, d), 7.69 (1H, t). Anal. Calcd for $C_{11}H_6F_6N_2O_4$: C, 38.39; H, 1.76; N, 8.14. Found: C, 38.33; H, 1.70; N, 8.26.

This compound was also synthesized by acylation of 2,6-diaminobenzoic acid using trifluoroacetic anhydride in a similar method described below to afford the product in 51% yield based on the amine.

*2,6-(n-BuCONH)$_2$C$_6$H$_3$COOH (**L6**).* 2,6-$(CH_3CONH)_2C_6H_3COOH$ (**L3**) (1.27 g, 5.35 mmol) was suspended in a 10% HCl aqueous solution (170 mL). After stirring for 30 min at 90 °C, the suspension changed to a pale yellow solution. This solution was dried in vacuo to give a white powder, 2,6-$(NH_2)_2C_6H_3COOH{\cdot}2HCl$. To the suspension of the powder in CH_2Cl_2 (30 mL) was added triethylamine (1.5 mL, 10.8 mmol); the mixture was cooled in an ice bath, and the color of the mixture turned yellow. Valeryl chloride (1.3 mL, 10.9 mmol) was added carefully to the mixture cooling in an ice bath, and a white powder was separated out immediately. After stirring overnight, insoluble materials were removed by filtration, and the filtrate was extracted with a 1 M NaOH aqueous solution. The aqueous layer was acidified by concentrated HCl and extracted with ethyl acetate. The organic layer was washed with a saturated NaCl aqueous solution and then dried over Na_2SO_4. After the solvents were removed, the residual

dx.doi.org/10.1021/ic400671v | *Inorg. Chem.* 2013, 52, 10812−10824

oil was crystallized from diethyl ether/*n*-hexane to give a white crystalline powder, which was recrystallized from ethyl acetate/*n*-hexane. Yield: 0.303 g (17.6%). ^{1}H NMR ($CDCl_3$): δ9.82 (2H, s), 8.14 (2H, d), 7.49 (1H, t), 2.40 (4H, t), 1.70 (4H, quin), 1.39 (4H, sex), 0.93 (6H, t). ESI-MS (methanol solution, negative mode): m/z 319.1 ($M-H^+$, calcd. 319.2), 661.1 ($2M-2H^++Na^+$, calcd. 661.3). Anal. Calcd for $C_{17}H_{24}N_2O_4$: C, 63.73; H, 7.55; N, 8.74. Found: C, 63.51; H, 7.48; N, 8.75.

*[Mg(O$_2$C-2-CH$_3$CONHC$_6$H$_4$)$_2$(H$_2$O)$_4$] (**1**).* To a methanol/water (1:1) solution (2 mL) of 2-$CH_3CONHC_6H_4COOH$ (**L1**) (142.5 mg, 0.80 mmol) was added a methanol/water (1:1) solution (1 mL) of $Mg(OAc)_2\cdot4H_2O$ (86.3 mg, 0.40 mmol) at room temperature and the solution was dried in vacuo. To the residue was added 2 mL of methanol/water (1:1), and the solution was evaporated under reduced pressure. This process was repeated several times to remove acetic acid completely. The residue was recrystallized from hot water. Colorless opaque plates were precipitated from the solution upon slow cooling to room temperature. Yield: 96.3 mg (53.5%). Anal. Calcd for $C_{18}H_{24}MgN_2O_{10}$: C, 47.76; H, 5.34; N, 6.19. Found: C, 47.83; H, 5.24; N, 6.17.

*[Mg(O$_2$C-2-CF$_3$CONHC$_6$H$_4$)$_2$(CH$_3$OH)$_4$] (**2**).* To a solution (1 mL) of **L2** (52.5 mg, 0.23 mmol) in methanol was added $Mg(OAc)_2\cdot4H_2O$ (24.6 mg, 0.11 mmol) at room temperature and the solution was dried in vacuo. To the oily residue was added 1 mL of methanol, and the solution was evaporated to remove acetic acid completely. The oily residue was washed with *n*-hexane to give a powder, which was recrystallized from hot methanol. Colorless blocks were obtained by slowly cooling the solution. Yield: 4.66 mg (5.9%). Anal. Calcd for $C_{22}H_{26}F_6MgN_2O_{10}$: C, 42.84; H, 4.25; N, 4.54. Found: C, 41.28; H, 4.06; N, 4.68.

*[Mg(dmf)$_2$(H$_2$O)$_4$][O$_2$C-2,6-(CH$_3$CONH)$_2$C$_6$H$_3$]$_2$ (**3**).* $Mg(OAc)_2\cdot4H_2O$ (44.9 mg, 0.209 mmol) and $(NEt_4)(OAc)\cdot4H_2O$ (108.3 mg, 0.413 mmol) was dissolved in a mixture of methanol and water (1:1) (5 mL). **L3** (199 mg, 0.841 mmol) was dissolved in the solution. After evaporation of the solvents under reduced pressure, the resulting residue was dissolved in acetonitrile. Diethyl ether was added to the solution until the solution became turbid. After 2 weeks, brown solid was obtained. This was hardly soluble in acetonitrile or methanol. The solid was recrystallized from DMF/diethyl ether. After 1 week, colorless plates were obtained. Yield: 12.7 mg (4.9%). Anal. Calcd for $C_{60}H_{84}MgN_{10}O_{16}$: C, 47.17; H, 6.22; N, 11.79. Found: C, 47.14; H, 6.10; N, 11.83.

*[Mg{2,6-(CH$_3$CONH)$_2$C$_6$H$_3$COO}$_2$(H$_2$O)$_4$] (**4**).* To a hot methanol solution (5 mL) of $Mg(OAc)_2\cdot4H_2O$ (55.0 mg, 0.257 mmol) was added **L3** (123 mg, 0.519 mmol). A white precipitate was obtained immediately. After decantation, the residue was dissolved in a mixture of methanol and water (1:1). After 1 week, colorless blocks were obtained by slow evaporation of solvents at room temperature. Yield: 34.0 mg (23.4%). Anal. Calcd for $C_{22}H_{30}MgN_4O_{10}$: C, 46.62; H, 5.33; N, 9.88. Found: C, 46.48; H, 5.26; N, 9.87.

*[Mg(CH$_3$OH)$_6$][O$_2$C-2,6-(CF$_3$CONH)$_2$C$_6$H$_3$]$_2$ (**5**).* To a solution of $Mg(OAc)_2\cdot4H_2O$ (43.0 mg, 0.200 mmol) in methanol (3 mL) was added a solution of **L4** (138 mg, 0.401 mmol) in methanol (2 mL), and the solution was concentrated until the viscosity was increased. After 1 day, some colorless crystals were obtained. Yield: 50.0 mg (27.6%). Anal. Calcd for $C_{28}H_{34}F_{12}MgN_4O_{14}$: C, 37.25; H, 3.80; N, 6.21. Found: C, 32.32; H, 2.68; N, 6.83. (Anal. Calcd for $[Mg(H_2O)_6][O_2C\text{-}2,6\text{-}(CF_3CONH)_2C_6H_3]_2$: C, 32.27; H, 2.71; N, 6.84.) The results of X-ray analysis showed the presence of methanol, but elemental analysis indicated replacement of the coordinated methanol molecules by water.

*[Mg(H$_2$O)$_6$][O$_2$C-2,6-(t-BuCONH)$_2$C$_6$H$_3$]$_2$·H$_2$O (**6**·H$_2$O).* $Mg(OAc)_2\cdot4H_2O$ (54.7 mg, 0.255 mmol) and 2,6-(*t*-$BuCONH)_2C_6H_3COOH$ (**L5**) (165 mg, 0.516 mmol) were mixed in 15 mL of ethanol and warmed until it dissolved. After the removal of insoluble materials by filtration, the filtrate was concentrated under reduced pressure. The residue was dissolved in acetonitrile/methanol (2:1), and a drop of water was added for crystallization. After 1 day, yellow blocks were separated out. Yield: 56.0 mg (30.1%). Anal. Calcd for $C_{34}H_{60}MgN_4O_{15}$: C, 51.75; H, 7.66; N, 7.10. Found: C, 51.66; H, 7.58; N, 7.14.

*[Mg{O$_2$C-2,6-(n-BuCONH)$_2$C$_6$H$_3$}$_2$(H$_2$O)$_2$(CH$_3$OH)$_2$] (**7**).* To a solution (1 mL) of $Mg(OAc)_2\cdot4H_2O$ (18.4 mg, 0.086 mmol) in methanol was added a solution (1 mL) of **L6** (54.9 mg, 0.171 mmol) in methanol. After 5 days, colorless blocks were obtained by slow evaporation of solvents at room temperature. Yield: 59.8 mg (91.5%). Anal. Calcd for $C_{36}H_{58}MgN_4O_{12}$: C, 56.66; H, 7.66; N, 7.34. Found: C, 56.26; H, 7.61; N, 7.38.

*[Mg(O$_2$C-2-CH$_3$CONHC$_6$H$_4$)(H$_2$O)$_5$][O$_2$C-2-CH$_3$CONHC$_6$H$_4$] (**8**).* This compound was synthesized in a similar method described for **1**, except for recrystallization from boiling water. To a solution of **L1** (0.432 g, 2.41 mmol) in methanol (5 mL) was added $Mg(OAc)_2\cdot4H_2O$ (0.254 g, 1.18 mmol) to give a white precipitate immediately. All solvents were removed under reduced pressure, and then the residue was recrystallized from boiling water to afford pale-yellow blocks. Yield: 0.295 g (52.9%). Anal. Calcd for $C_{18}H_{26}MgN_2O_{11}$: C, 45.93; H, 5.57; N, 5.95. Found: C, 45.90; H, 5.41; N, 5.94.

Physical Measurements. ^{1}H nuclear magnetic spectroscopy (^{1}H NMR) spectra were obtained on a JEOL JNM-EX270 spectrometer, using $CDCl_3$ solution at 30 °C. Electron spin ionization-mass spectroscopy (ESI-MS) spectra were taken on a Finnigan MAT LCQ spectrometer, using methanol solution in positive and negative modes.

X-ray Analysis. Each single crystal of compounds **1**−**8** was mounted in a loop with Nujol. The X-ray data were collected at 200 K on a Rigaku Raxis-RAPID Imaging Plate diffractometer with graphite monochromated Mo Kα radiation (λ = 0.71075 Å). The structures were solved via a direct method (SIR92,[32] SHELXS-97[33]) and expanded Fourier techniques using SHELXL-97.[33] Non-hydrogen atoms were refined anisotropically. H atoms of amide and OH groups were found in the differential Fourier map, then located there, and their coordinates were refined. Because the N−H distances in **8** did not converge to reasonable values, these NH protons were treated as riding models. The other H atoms were generated by the riding and rotating model in SHELXL-97.

Density Functional Theory (DFT) Calculations. Geometry optimizations and natural bond orbital (NBO) analysis were performed using Becke's three-parameter hybrid functionals (B3LYP) in the Gaussian 03 program package,[34] using the 6-31+G** basis set. The initial structure of model **A** was constructed by using internal coordinates based on the X-ray structure of $[Mg(O_2C\text{-}2\text{-}CH_3CONHC_6H_4)_2(H_2O)_4]$ (**1**). The geometrical parameters of model **B** are the same as those of model **A**, except for the use of flipped aromatic ring about the phenyl−COO bond. For model **C**, the amide groups of model **A** were replaced by H atoms with normal C−H distance. The coordinates of **8** were used for the cationic initial model **D**, $[Mg(O_2C\text{-}2\text{-}CH_3CONHC_6H_4)(H_2O)_5]^+$. Analogous models **E** (flipped aromatic ring) and **F** (without amide group) were derived from **D**, as described above for **A**−**C**. Initial structures of *cis*-coordinated models, *cis*-$[Mg(O_2C\text{-}2\text{-}CH_3CONHC_6H_4)_2(H_2O)_4]$ (**G**, **H**, **J**) and *cis*-$[Mg(O_2CC_6H_5)_2(H_2O)_4]$ (**I**), were prepared by some modifications of the X-ray structure of $[Mg\{O_2C\text{-}2,6\text{-}(n\text{-}BuCONH)_2C_6H_3\}_2(H_2O)_2(CH_3OH)_2]$ (**7**). The substituent groups and methanol were replaced by suitable groups. The structures were roughly optimized using the 3-21G* basis set and reoptimized by using the higher-level basis set described above. The optimized geometry was analyzed by MolStudio R4.0 (NEC Corp., Japan).

RESULTS

Synthesis. Magnesium complexes were synthesized using a ligand-exchange reaction between magnesium acetate and the corresponding carboxylic acid. Exhaustive evaporation of free acetic acid under reduced pressure completed the reaction. Trials of recrystallization using different solvents afforded suitable crystals for the X-ray analysis. The products were isolated as single crystals, resulting in relatively low yields. The low solubility of the complexes in nonpolar solvents and the

dx.doi.org/10.1021/ic400671v | Inorg. Chem. 2013, 52, 10812−10824

Table 1. Crystallographic Data for Compounds 1−4

	1	2	3	4
formula	$C_{18}H_{24}MgN_2O_{10}$	$C_{22}H_{26}F_6MgN_2O_{10}$	$C_{28}H_{44}MgN_6O_{14}$	$C_{22}H_{30}MgN_4O_{12}$
fw	452.70	616.75	712.99	566.80
cryst syst	triclinic	monoclinic	monoclinic	triclinic
space group	$P\bar{1}$	$C2/c$	$P2_1/c$	$P\bar{1}$
a (Å)	6.7274(9)	22.358(2)	14.285(1)	7.581(2)
b (Å)	9.090(1)	9.5203(7)	5.2966(5)	8.289(3)
c (Å)	9.865(1)	13.724(1)	23.179(2)	11.245(4)
α (deg)	111.785(3)	90	90	70.87(2)
β (deg)	102.010(3)	106.966(2)	100.963(7)	75.99(2)
γ (deg)	95.572(3)	90	90	79.86(2)
V (Å^3)	537.8(1)	2793.5(4)	1721.8(3)	644.1(3)
Z	1	4	2	1
d_{calc} (g cm^{-3})	1.398	1.466	1.375	1.461
μ (mm^{-1})	0.139	0.159	0.126	0.140
goodness of fit, GOF	1.13	1.14	1.02	1.05
$R1^a$ [$I > 2\sigma(I)$]	0.054	0.046	0.079	0.039
$wR2^b$ (all data)	0.162	0.138	0.218	0.102

$^aR1 = \sum||F_0| - |F_c||/\sum|F_0|$. $^bwR2 = \{\sum[w(F_0^2 - F_c^2)^2]/\sum[w(F_0^2)^2]\}^{1/2}$.

Table 2. Crystallographic Data for Compounds 5−8

	5	6·H_2O	7	8
formula	$C_{28}H_{34}F_{12}MgN_4O_{14}$	$C_{34}H_{60}MgN_4O_{15}$	$C_{36}H_{58}MgN_4O_{12}$	$C_{18}H_{26}MgN_2O_{11}$
fw	902.88	789.17	763.18	470.72
cryst syst	triclinic	monoclinic	orthorhombic	triclinic
space group	$P\bar{1}$	$P2_1/c$	$Pbcn$	$P1$
a (Å)	9.781(6)	12.241(3)	10.0683(8)	6.954(2)
b (Å)	10.393(7)	15.512(4)	17.625(1)	14.566(7)
c (Å)	10.999(9)	27.609(7)	23.070(2)	22.183(8)
α (deg)	102.82(3)	90	90	100.40(1)
β (deg)	107.57(2)	126.45(1)	90	94.05(1)
γ (deg)	112.72(2)	90	90	101.22(1)
V (Å^3)	907(1)	4216(1)	4093.8(5)	2154(5)
Z	1	4	4	4
d_{calc} (g cm^{-3})	1.652	1.243	1.238	1.451
μ (mm^{-1})	0.183	0.110	0.106	0.146
goodness of fit, GOF	1.07	1.04	1.08	1.00
$R1^a$ [$I > 2\sigma(I)$]	0.055	0.047	0.068	0.060
$wR2^b$ (all data)	0.143	0.120	0.199	0.164

$^aR1 = \sum||F_0| - |F_c||/\sum|F_0|$. $^bwR2 = \{\sum[w(F_0^2 - F_c^2)^2]/\sum[w(F_0^2)^2]\}^{1/2}$.

labile magnesium−carboxylate bonds prevented us from determining the solution structures via NMR spectroscopy. Evaluation of the strength of the NH···O hydrogen bonds failed because only broad, overlapped, and complicated infrared (IR) spectra were obtained in the ν(NH) and ν(OH) regions. Therefore, the discussions in this report are limited to the structural consideration using X-ray analysis and theoretical calculations. Eight molecular structures were determined by X-ray analysis and the crystallographic data are listed in Tables 1 and 2.

Structures of Magnesium Carboxylates Containing Single NH···O Hydrogen Bond. Molecular structures of $[Mg(O_2C\text{-}2\text{-}CH_3CONHC_6H_4)_2(H_2O)_4]$ (**1**) and $[Mg(O_2C\text{-}2\text{-}CF_3CONHC_6H_4)_2(CH_3OH)_4]$ (**2**) are shown in Figure 2. H atoms, except for those in the NH and OH groups, are omitted for the sake of clarity. Red dotted lines represent possible NH···O hydrogen bonds. These molecules were crystallized in a centrosymmetric space group and each Mg ion was found on an inversion center with mutually *trans* carboxylate ligands.

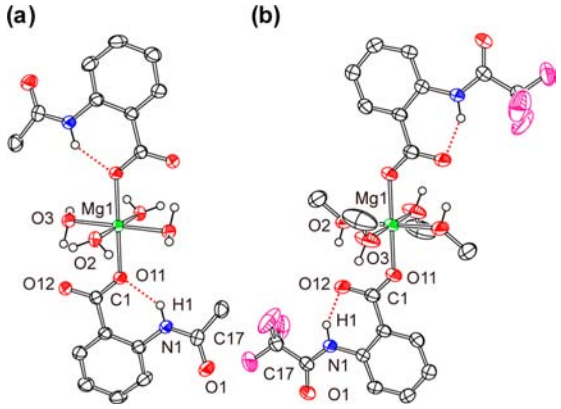

Figure 2. Molecular structures of (a) **1** and (b) **2**.

Although the number of reported structures of mononuclear magnesium dicarboxylates is very limited, a *trans* configuration is typical for the analogous complexes; e.g., [Mg-

dx.doi.org/10.1021/ic400671v | Inorg. Chem. 2013, 52, 10812−10824

$(O_2CCH_3)_2(H_2O)_4]$,[35] $[Mg(O_2C\text{-}4\text{-}NO_2C_6H_4)_2(CH_3OH)_4]$, and $[Mg(O_2C\text{-}4\text{-}CH_3C_6H_4)_2(CH_3OH)_4]$.[36] The Mg ion resides in the plane of the carboxylate group in a *syn* conformation that is preferable to a stable bond.[37]

Interestingly, the modes of the intramolecular NH···O hydrogen bonds in **1** and **2** are very different from each other. In **1**, the amide group (NH) is hydrogen-bonded to the coordinated oxygen atom (O11). However, NH in **2** was directed to the uncoordinated carbonyl oxygen atom (O12). The two distinct hydrogen-bonding modes significantly influenced the character of the Mg−O bond. Some selected bond distances and angles are listed in Table 3. The Mg−O

Table 3. Selected Bond Distances and Bond Angles for 1 and 2

	1	2
Bond Distances (Å)		
Mg1−O11	2.073(2)	2.031(2)
Mg1−O2	2.071(2)	2.067(2)
Mg1−O3	2.099(2)	2.095(2)
mean Mg−O (water)	2.085	
mean Mg−O (methanol)		2.081
C1−O11	1.270(3)	1.259(3)
C1−O12	1.255(3)	1.268(3)
N1−H1	0.88(3)	0.88(3)
C17═O1	1.243(3)	1.224(3)
H1···O11 (O12)	1.89(3)	1.79(3)
Bond Angles (deg)		
Mg1−O11−C1	129.8(2)	134.0(2)
N1−H1−O11 (O12)	139(3)	147(3)

(carboxylate) distances for $[Mg(O_2CCH_3)_2(H_2O)_4]$[35] and $[Mg(O_2C\text{-}4\text{-}CH_3C_6H_4)_2(CH_3OH)_4]$[36] have been reported as 2.0761(8) and 2.061(2) Å, respectively. Considering these distances, the Mg−O distance in **1** (2.073(2) Å) can be considered as normal or slightly long. In contrast, **2** has a significantly shorter Mg−O bond (2.031(2) Å). Similar NH···O hydrogen bonds in the latter mode have been widely found in the active sites of metalloproteins containing metal−carboxylate bonds.[3,5,38,39] These results suggest that hydrogen bonding to the uncoordinated carbonyl oxygen stabilizes the Mg−O bond. However, a direct hydrogen bond to the coordinated oxygen decreases electron donation to the Mg ion, thus resulting in a relatively weak Mg−O bond. The longer Mg−O bond and smaller Mg−O−C angle in **1** indicate more p-character in the O atom than in **2**, suggesting that hybridization of s and p orbitals was altered to supply an additional bond to the neighboring NH group. All of the H atoms from the water molecules were found in the differential Fourier map, whose positions were then refined. The OH groups were intramolecularly or intermolecularly hydrogen-bonded to the carbonyl O atoms.

Synthesis of Magnesium Complexes with Carboxylate Containing Double NH···O Hydrogen Bonds. Benzoate derivatives containing intramolecular double NH···O hydrogen bonds and their calcium complexes have been reported in previous papers.[27,31] The molecular structure of 2,6-$(CH_3CONH)_2C_6H_3COOH$ (**L3**) with the crystallographic data is shown in Figure S1 and Table S1 in the Supporting Information. The structure resembles the one reported for 2,6-$(t\text{-}BuCONH)_2C_6H_3COOH$ (**L5**), except for the presence of a hydrogen bond from the acidic OH to the crystal water. Attempts to synthesize an anionic magnesium complex analogous to the calcium derivatives failed and resulted in a neutral and/or solvated complex. Such differences of the coordination modes between Mg^{2+} and Ca^{2+} ions have already been predicted using theoretical calculations of the protein matrix by Lim et al., which shows Ca^{2+} ion prefers to bind to the third carboxylate rather than bidentately but Mg^{2+} ion chooses the formation of a hydrated neutral complex.[40] All the magnesium complexes in this Article contain two or less carboxylate ligands with octahedral geometry. This tendency is in good agreement with the reported systematic calculations.[41−44] Magnesium acetate was mixed with four equivalents of **L3** in the presence of 2 equiv of $(NEt_4)(OAc)$, resulting in a precipitate, which was recrystallized from DMF to give the solvated compound $[Mg(dmf)_2(H_2O)_4][O_2C\text{-}2,6\text{-}(CH_3CONH)_2C_6H_3]_2$ (**3**). The molecular structure is shown in Figure 3a, and geometrical parameters are listed in Table S2

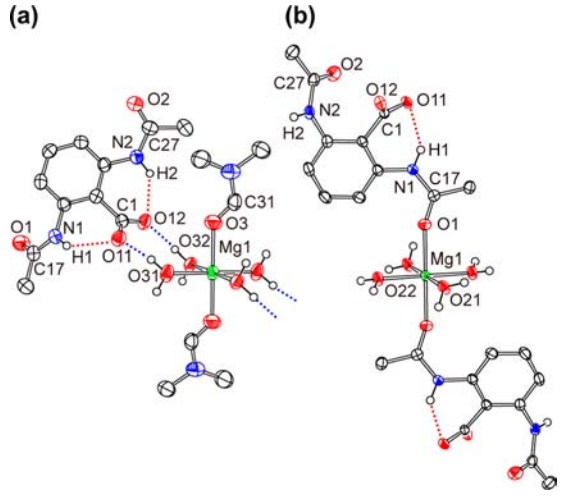

Figure 3. Molecular structures of (a) **3** and (b) **4**.

in the Supporting Information. The Mg ion is coordinated to two carbonyl groups of DMF and four water molecules. The Mg−O (DMF) distance and Mg−O═C angle are in the range of the previously reported values.[45,46] The deprotonated **L3** is not directly coordinated to the Mg ion; instead, it interacts with the coordinated water via OH···O hydrogen bonds, which are shown as blue dotted lines. The carboxylate anion forms intramolecular double NH···O hydrogen bonds (red dotted lines) and the carboxylate negative charge is delocalized in the extended conjugated system of the amide carbonyl group. The amide planes deviate from the benzene ring with torsion angles of 48.1(6)° (around N1−C) and 20.0(7)° (around N2−C). The carboxylate group is out of the plane of the aromatic ring with a dihedral angle of −48.2(5)°. The lack of coplanarity suggests that the hydrogen bonds are not very strong. The complex apparently forms a soft acid−soft base structure connected by hydrogen bond chains, where the hydrated Mg ion behaves like a soft acid and the carboxylate acts as a weak soft base.

When DMF was not used to avoid coordination, a neutral compound, $[Mg\{2,6\text{-}(CH_3CONH)_2C_6H_3COO\}_2(H_2O)_4]$ (**4**), was obtained. The molecular structure of **4** is shown in Figure 3b. Surprisingly, the amide carbonyl group of **L3** was coordinated to the Mg ion, disregarding the carboxylate anion. Selected bond distances and angles are summarized in

dx.doi.org/10.1021/ic400671v | *Inorg. Chem.* 2013, 52, 10812−10824

Table S3 in the Supporting Information. One (H1) of the two protons of the amide groups is hydrogen-bonded to the carboxylate oxygen (O11). The other NH (H2) is intermolecularly hydrogen-bonded to O12. The relatively long Mg1−O1 distance (2.075(1) Å) and large Mg1−O1−C17 angle (152.6(1)°) indicate an ionic bond character or the presence of significant charge-transfer interaction.[47] These results suggest that the carboxylate ligand, with double NH···O hydrogen bonds, acts as a soft base. Therefore, it would not coordinate directly to a hard Mg ion. Such overwhelming coordination of the amide group in the presence of a carboxylate ligand has been shown only in a few reports.[48,49] The mean distance of the Mg−O (water) bonds is 2.049 Å, which is shorter than that of **1** (2.085 Å) and **3** (2.077 Å). These results indicate the donation of water to the electron-deficient Mg ion is increased by the small electron donation of the carbonyl ligand.

The reaction between magnesium acetate and another carboxylic acid, 2,6-$(CF_3CONH)_2C_6H_3COOH$ (**L4**) or **L5**, gave salts of the fully solvated Mg ion and carboxylate anions. The molecular structures, $[Mg(CH_3OH)_6][O_2C\text{-}2,6\text{-}(CF_3CONH)_2C_6H_3]_2$ (**5**) and $[Mg(H_2O)_6][O_2C\text{-}2,6\text{-}(t\text{-}Bu\text{-}CONH)_2C_6H_3]_2$ (**6**), are shown in Figure 4. Selected bond

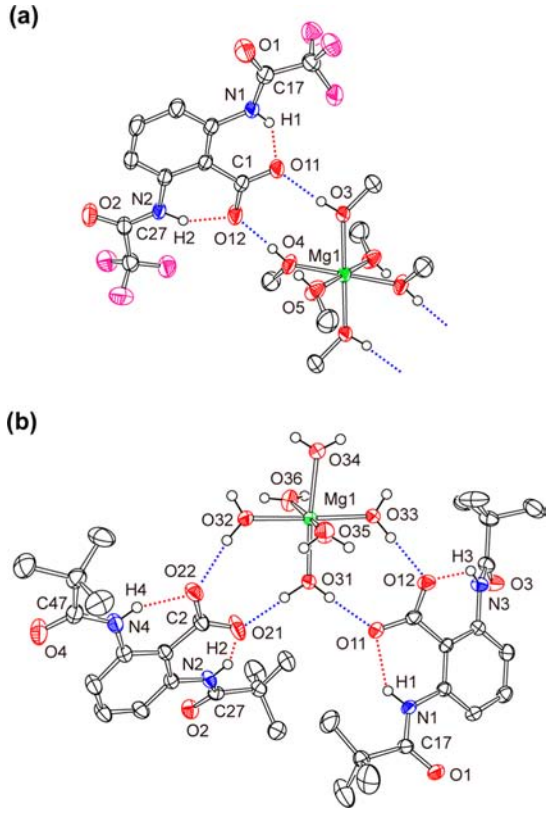

Figure 4. Molecular structures of (a) **5** and (b) **6**.

distances and angles are listed in Tables S4 and S5 in the Supporting Information. The carboxylate anions form intramolecular NH···O hydrogen bonds (red dotted lines) and interionic OH···O hydrogen bonds (blue dotted lines) with the OH group of the coordinated water or methanol. Two carboxylate anions are located in the *trans* and *cis* configurations for **5** and **6**, respectively. Salts of $[Mg(H_2O)_6]^{2+}$ with carboxylate anions have been reported in both aliphatic[50] and aromatic[51] carboxylates.

The deprotonated anion of **L4** has a substantially planar structure with the torsion angles of −2.2(4)° (around N1−C) and 11.4(4)° (around N2−C), and it forms strong intramolecular NH···O hydrogen bonds with short H···O distances (1.73(3) and 1.80(2) Å). Electron-withdrawing CF_3 groups increase the acidity of the NH proton, resulting in the preferable strong hydrogen bonds. The electronegative CF_3 groups form interionic CH···F interactions with the methyl group of the coordinated methanol and intramolecular NH···F hydrogen bonds. All the OH groups of methanol are hydrogen-bonded with either the carboxylate anion (O3H···O11, O4H···O12) or carbonyl group (O5H···O1). The equivalent C1−O11 and C1−O12 distances indicate a typical conjugated form of the carboxylate anion. The conjugation is expanded to the hydrogen bond chain, including the π-system of the amide plane, O5−H···O1−C17−NH···O11···H−O3.

The coordinated water molecules are intermolecularly hydrogen-bonded in the crystal of **6**·H_2O. The water molecules are classified into four categories according to the number and types of functional groups with which the molecules interact: the first (O31) interacts with two carboxylate anions; the second (O32, O33) interacts with one carboxylate anion and one carbonyl group; the third (O34, O36) with two carbonyl groups; and the fourth (O35) with two crystal water molecules. The electron density of the coordinated oxygen atom is probably increased by the formation of an OH···O hydrogen bond with the electron-rich carboxylate anion, increasing the basicity of the water ligand. Electron donation through the hydrogen bond should follow the order of carboxylate > carbonyl. This estimation is consistent with the observed result. The Mg−O31 (2.014(1) Å) bond with two OH···O (carboxylate) is the shortest. On the other hand, the Mg−O32 (2.044(1) Å) and Mg−O33 (2.031(1) Å) bonds with one OH···O (carboxylate) are significantly shorter than the other Mg−O (2.081(1), 2.100(1) Å) bond. The mean Mg−O (water) distance (2.062 Å) is significantly shorter than that of **1**, which indicates that the coordination of carboxylate anion increases the electron density on the Mg^{2+} ion resulting the decrease of the donation from the aquo ligand.

Many trials to synthesize *trans*-bis(carboxylate) magnesium complex using the doubly NH···O hydrogen-bonded carboxylate ligands failed even if strictly dehydrated solvents were used. This fact strongly suggests that the carboxylate anion with double NH···O hydrogen bonds is unusually weak Lewis base. Only one example with direct coordination of the ligand was obtained, which is described below.

Structure of *Cis*-Coordinated Magnesium Carboxylate. The magnesium complex $[Mg\{O_2C\text{-}2,6\text{-}(n\text{-}Bu\text{-}CONH)_2C_6H_3\}_2(H_2O)_2(CH_3OH)_2]$ (**7**) was successfully obtained when 2,6-$(n$-BuCONH$)_2C_6H_3$COOH (**L6**) was used. The molecular structure is shown in Figure 5 and selected geometrical parameters are listed in Table 4. The molecule has a crystallographic 2-fold axis. Interestingly, two carboxylate ligands are coordinated in the *cis* configuration. Such a *cis* isomer is unusual for synthetic magnesium carboxylates and previously has been seen only in chelate compounds[52−54] and catena structures.[55−57] However, the *cis* configuration is popular in biological systems.[3,5,38] The *n*-butyl chain is close to the benzoate moiety via intra- and intermolecular CH···π interactions with short bond distances (C_γ−H···C11 = 2.95 Å and C_α−H···C16 = 2.87 Å, respectively). These stacking interactions probably stabilize the *cis* configuration.

dx.doi.org/10.1021/ic400671v | *Inorg. Chem.* 2013, 52, 10812−10824

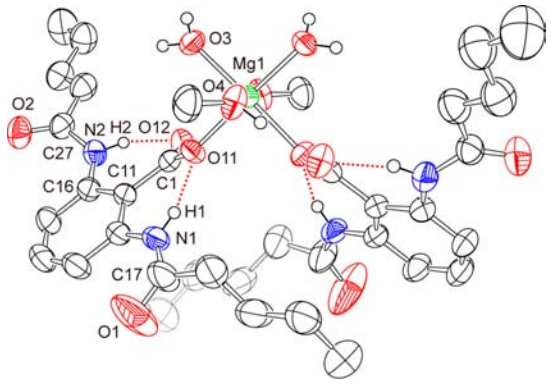

Figure 5. Molecular structure of **7**.

Table 4. Selected Bond Distances and Bond Angles for 7

Bond Distance Measurements	
atom pair	bond distance
Mg1−O11	2.079(2) Å
Mg1−O3	2.038(3) Å
Mg1−O4	2.062(3) Å
C1−O11	1.268(4) Å
C1−O12	1.257(4) Å
N1−H1	0.82(4) Å
N2−H2	0.86(4) Å
C17═O1	1.220(5) Å
C27═O2	1.217(5) Å
H1···O11	1.89(5) Å
H2···O12	1.93(5) Å
Bond Angle Measurements	
bond angle	value
Mg1−O11−C1	133.0(2)°
N1−H1−O11	147(4)°
N2−H2−O12	135(4)°

The relatively long Mg−O11 (2.079(2) Å) bond indicates the low basicity of the carboxylate ligand, which is caused by the double intramolecular NH···O hydrogen bonds (H1···O11 = 1.89(5) Å, H2···O12 = 1.93(5) Å). In contrast, the water ligand at the *trans* position shows a short Mg−O3 bond (2.038(3) Å). These results suggest that the strong coordination of a water molecule alters a hard Mg ion to a softer hydrated Mg ion. The softer ion then becomes more attractive to the exceedingly soft doubly hydrogen-bonded carboxylate ligand. From an opposite point of view, the doubly hydrogen-bonded ligand strengthens the coordination of the water molecule at the *trans* position.

Coordination of a Water Molecule *Trans* to the Carboxylate Ligand. Recrystallization of **1** from boiling water gave a partially hydrated compound $[Mg(O_2C\text{-}2\text{-}CH_3CONHC_6H_4)(H_2O)_5][O_2C\text{-}2\text{-}CH_3CONHC_6H_4]$ (**8**). The molecular structure and crystal packing are shown in Figure 6. Four molecules (1−4) were found in the asymmetric unit, whose geometrical parameters are summarized in Table 5. In comparison with **1**, an additional water molecule was coordinated in place of the carboxylate ligand, and the dissociated anion was located nearby via OH···O hydrogen bonds in **8**. The position of the NH···O hydrogen bond is very similar to that of **1**, with regard to the coordinated carboxylate. The geometrical parameters of molecules 1−4 either resemble each other or are essentially identical. The Mg−O (carboxylate)

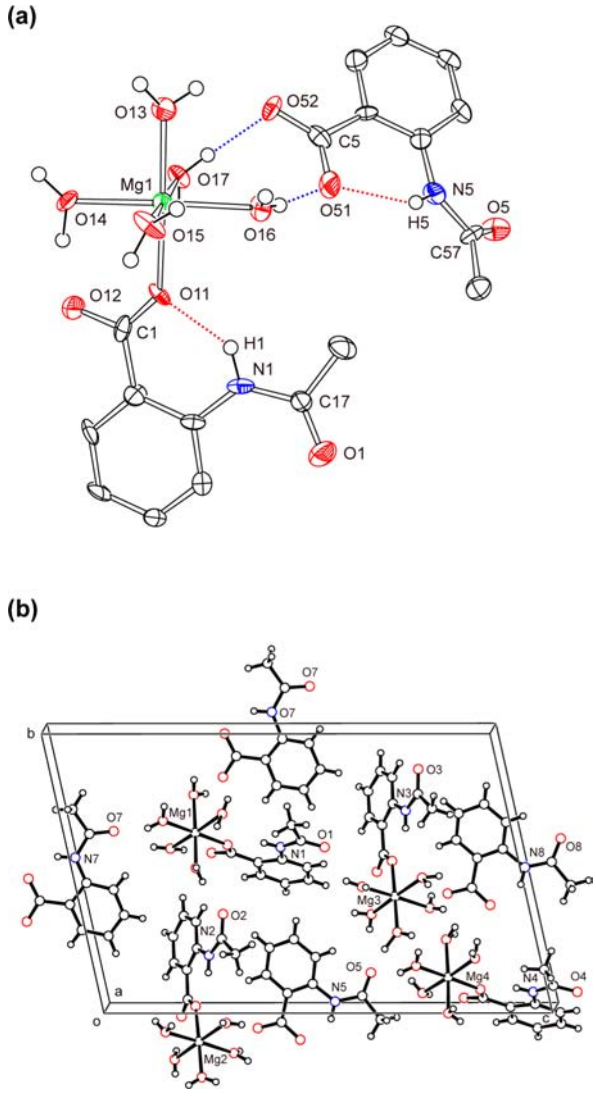

Figure 6. (a) Molecular structure for one (molecule 1) of the four molecules of **8** in the asymmetric unit and (b) the crystal packing in the unit cell.

distances of **8** are within the range 2.047—2.050 Å and the Mg−O−C angles are in the range 134.9°—137.7°, which are shorter distances and wider angles compared to **1**. The Mg−O (water) distance *trans* to the carboxylate ligand is 2.037 Å (mean), which is comparable to **7**. These results suggest that strong coordination of water molecules strengthens the Mg−carboxylate bond at the *trans* position. Similar contributions are also seen in the structure of **7**. The water ligand of **7** permits the coordination of a very weakly basic, doubly hydrogen-bonded carboxylate. In the case of **8**, the water ligand strengthens the slightly weak Mg−carboxylate bond to give a normal bond. The mean Mg−O (water) distances (2.065—2.071 Å) are between those of **1** (2.085 Å) and **6** (2.062 Å), which is simply interpreted as the dependence on the number of carboxylate ligands.

DISCUSSION

Contribution of NH···O Hydrogen Bonds to Mg−O Bonds. To determine the contribution of the NH···O hydrogen bonds to the magnesium−carboxylate bonds found in the structures of **1** and **2**, theoretical calculations were done

dx.doi.org/10.1021/ic400671v | *Inorg. Chem.* 2013, 52, 10812−10824

Table 5. Selected Bond Distances and Bond Angles for 8

	molecule 1 (n = 1)	molecule 2 (n = 2)	molecule 3 (n = 3)	molecule 4 (n = 4)
		Bond Distance Measurements		
Mgn–On1	2.049(6) Å	2.050(6) Å	2.048(6) Å	2.047(6) Å
Mgn–On3 (*trans*)	2.041(6) Å	2.038(6) Å	2.039(6) Å	2.028(7) Å
Mgn–On4 (*cis*)	2.077(6) Å	2.076(6) Å	2.083(6) Å	2.078(6) Å
Mgn–On5 (*cis*)	2.026(5) Å	2.081(6) Å	2.088(6) Å	2.064(7) Å
Mgn–On6 (*cis*)	2.092(6) Å	2.087(6) Å	2.102(6) Å	2.092(6) Å
Mgn–On7 (*cis*)	2.091(6) Å	2.072(6) Å	2.031(7) Å	2.089(6) Å
mean Mg–O (warer)	2.065 Å	2.071 Å	2.069 Å	2.070 Å
Cn–On1	1.25(1) Å	1.27(1) Å	1.27(1) Å	1.29(1) Å
Cn–On2	1.284(9) Å	1.25(1) Å	1.27(1) Å	1.24(1) Å
Cn7═On	1.22(1) Å	1.22(1) Å	1.22(1) Å	1.23(1) Å
Hn···On1[a]	1.92 Å	1.91 Å	1.89 Å	1.91 Å
		Bond Angle Measurements		
Mgn–On1–Cn	137.2(5)°	135.5(5)°	135.2(6)°	134.9(5)°
Nn–Hn–On1[a]	139°	138°	139°	139°

[a]Nn–Hn = 0.88 Å (fixed).

using density functional theory (DFT). Based on the molecular structure of **1**, simplified centrosymmetric models, **A**–**C**, were constructed, as shown in Figure 7a, and geometrically optimized structures were obtained (Figure 7b). Isomeric models, **A** and **B**, of $[Mg(O_2C\text{-}2\text{-}CH_3CONHC_6H_4)_2(H_2O)_4]$, simulate the two modes of NH···O hydrogen bonds found in structures **1** and **2**, respectively. Model **C** is a nonsubstituted benzoate complex, $[Mg(O_2CC_6H_5)_2(H_2O)_4]$. The calculated geometric and electrostatic parameters are listed in Table 6. The Wiberg bond index and atom–atom overlap-weighted natural atomic orbital (NAO) bond order are shown in order to estimate the covalency of the bond. For normal covalent bonds, the bond index is approximately equal to the conventional bond order. Positive values of atom–atom overlap-weighted NAO bond order indicate a bonding character or an attractive interaction between the two atoms.

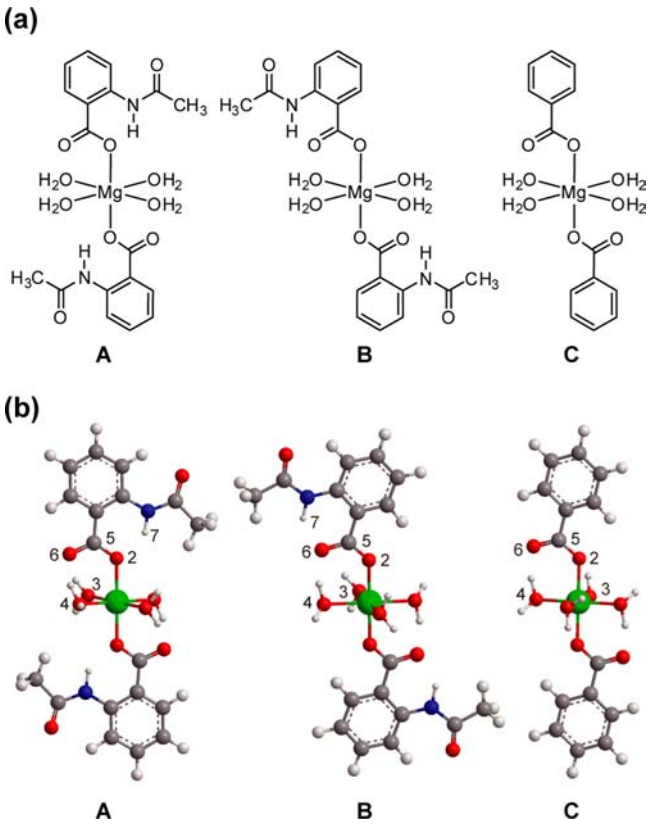

Figure 7. (a) Schematic drawing of initial models **A**–**C** for the DFT calculations. (b) Optimized structures of models **A**–**C**.

Table 6. Geometric and Electrostatic Parameters of the Optimized Structures of Models A–C

	A	B	C
Mg–O2 (Å)	2.0614	2.0335	2.0434
bond index[a]	0.1831	0.2021	0.1995
bond order[b]	0.2785	0.3121	0.3173
Mg–O3 (Å)	2.1344	2.1666	2.1724
bond index	0.1509	0.1392	0.1375
bond order	0.2221	0.2252	0.2272
Mg–O4 (Å)	2.1408	2.1057	2.0998
bond index	0.1510	0.1639	0.1664
bond order	0.2200	0.2619	0.2681
mean Mg–O (water)	2.1376	2.1362	2.1361
C5–O2 (Å)	1.2891	1.2796	1.2846
bond index	1.3124	1.3373	1.3204
bond order	0.9897	1.0092	0.9971
C5–O6 (Å)	1.2721	1.2740	1.2610
bond index	1.4042	1.3977	1.4590
bond order	1.0291	1.0245	1.0444
H7···O2 (O6)	1.8001	1.7803	
bond index	0.0501	0.0567	
bond order	0.0666	0.0762	
Mg–O2–C5 (deg)	123.91	133.64	130.37
natural charge			
Mg	1.43187	1.42433	1.42581
O2	−0.82163	−0.81899	−0.83095
O6	−0.77535	−0.76021	−0.72457

[a]Wiberg bond index. [b]Atom–atom overlap-weighted NAO bond order.

dx.doi.org/10.1021/ic400671v | *Inorg. Chem.* 2013, 52, 10812–10824

The Mg−O2 distances clearly show an elongation in **A** and shortening in **B**, compared to **C**. Smaller (123.91°) and larger (133.64°) Mg−O2−C5 angles are also found in **A** and **B**, respectively, than that of **C**. These results are consistent with the experimental results from X-ray analysis. Although the bond lengths were in the expected order, the bond order was reversed for **B** and **C**, that is, the short Mg−O2 bond does not mean simply covalency. These results suggest that the shortening of the bond length of Mg−O2 in **B** was caused by another factor, which can be reasonably explained by considering the contribution of donor−acceptor interaction (i.e., delocalization of electrons). Second-order perturbative estimates of the charge-transfer interaction[58,59] from O2 to Mg for **A**−**C** using NBO basis are shown in Table 7. The major

Table 7. Second-Order Perturbative Estimates of Charge-Transfer Interaction from O2 to Mg in the NBO Basis for the Optimized Models A−C

donor NBO				
	hybrid	acceptor NBO	stabilization energy[a] (kcal mol^{-1})	total
		Model **A**		
n_O	$sp^{3.72}$	s^*_{Mg}	24.89	
		p^*_{Mg}	28.40	53.29
n_O	$sp^{1.43}$	s^*_{Mg}	6.86	
		p^*_{Mg}	12.64	
		p^*_{Mg}	2.32	21.82
n_O	p	p^*_{Mg}	2.52	
		Model **B**		
n_O	$sp^{2.66}$	s^*_{Mg}	27.39	
		p^*_{Mg}	30.29	57.68
n_O	$sp^{2.66}$	p^*_{Mg}	2.34	
	$sp^{1.94}$	s^*_{Mg}	6.71	
		p^*_{Mg}	9.69	
		p^*_{Mg}	5.33	24.07
n_O	p	p^*_{Mg}	3.02	
		Model **C**		
n_O	$sp^{2.5}$	s^*_{Mg}	27.05	
		p^*_{Mg}	29.34	56.39
n_O	$sp^{2.5}$	p^*_{Mg}	3.95	
	$sp^{1.98}$	s^*_{Mg}	5.73	
		p^*_{Mg}	8.21	
		p^*_{Mg}	5.99	23.88
n_O	p	p^*_{Mg}	2.49	

[a]Selected energies were shown >2 kcal mol^{-1}.

interactions $n_O \rightarrow s^*_{Mg}$ and $n_O \rightarrow p^*_{Mg}$ are found, which show significant stabilization energy. When the molecules (or Mg−O2 bonds) are placed along the *z*-axis (the vertical axis in Figure 7), the dominant contribution comes from the filled p_z-rich hybrid on the oxygen atom (sp^n, $n > 2$) interacting with vacant s* or p_z* orbitals on the Mg ion. The delocalization of electrons occurs along the O−Mg bond as σ-type donation. The total stabilization energy (expressed in units of kcal mol^{-1}) ranks in the following order: **B** (57.68) > **C** (56.39) > **A** (53.29). The other donations from the hybrid orbital are π-type mixed with σ-type in the same order: **B** (24.07) > **C** (23.88) > **A** (21.82). Small contributions from $p\pi(O) \rightarrow p\pi^*(Mg)$ donation show the following order: **B** (3.02) > **A** (2.52) > **C** (2.49). The donation decreased both the negative charge on O2 and the positive charge on Mg, as shown in Table 6.

The difference in the bond distances between C5−O2 and C5−O6 of **B** is very small (0.0056 Å), indicating that the resonance structure of the carboxylate moiety is likely in a bidentate coordination mode. However, **A** and **C** show significantly longer C5−O2 bonds. These results are consistent with the observed structures of **2** and **1**. The resonance structure of the carboxylate anion is extended through the entire ligand, including the NH···O═C hydrogen bond, which probably helped stabilize the relatively short Mg−O bond.

Influence of the Magnesium−Carboxylate Bond on the Mg−O Bond at the *Trans* Position. Magnesium bis(carboxylate) complexes are usually present as *trans* isomers in crystal. As found in the structure of **1**, a direct NH···O hydrogen bond to the coordinated oxygen atom weakened the Mg−O bond by decreasing the electron density on oxygen and lowering the basicity of the ligand. Conversely, hydrogen bond to the uncoordinated carbonyl oxygen shortened the Mg−O bond. Introducing double hydrogen bonds to the carboxylate ligand decreased the basicity of both the oxygen atoms, resulting in weak coordination power; therefore, any magnesium complex with such ligands could not be isolated as a *trans* isomer. Fortunately, the coordination of such a weak Lewis base was found solely in the *cis* configuration of **7**. The weak coordination of a doubly hydrogen-bonded carboxylate ligand is supported by strong donation from a water molecule at the *trans* position. Generally, the *trans* influence in coordination complexes is attributed to transition-metal complexes containing d-electrons and $d\pi-p\pi$ interactions.[23] In elements with only s and p electrons, such interaction has rarely been considered, because of the limited orientation of these orbitals. Instead, traditional hard and soft acid and base (HSAB) theory is used. The Mg ion is a hard acid and prefers hard bases, including ordinary carboxylate.[60] When a water molecule strongly coordinates to a naked Mg ion, the positive charge on the ion spreads over the coordinated water, forming a polarizable $[Mg(H_2O)_m]^{2+}$ ($1 \leq m \leq 6$) ion. This ion probably acts as a relatively soft acid. When $m = 6$, the Mg^{2+} ion is a fully hydrated ion covered by H_2O; thus, it never coordinates directly to the carboxylate ligand, as found in **6**.

When $m = 5$, one vacant site of the $[Mg(H_2O)_5]^{2+}$ ion accepts the carboxylate ligand with a normal Mg−O distance, as seen in the crystal of **8**. The Mg−O11 (carboxylate) bond is shorter than that of **1** and the Mg−O13 (water) distance (2.041(6) Å) at the *trans* position is relatively short among the Mg−O (water) bonds (mean = 2.065 Å). These facts are attributable to the *trans* influence, which was examined by theoretical calculations. The initial models—the anion part of **8** (**D**), the flipped aromatic ring of **D** (**E**), and without the amide group (**F**)—were used for DFT calculations (see Figure 8). The parameters obtained by geometry optimizations are listed in Table S6 in the Supporting Information. The directly hydrogen-bonded Mg−O2 bond of **D** (2.0275 Å) is longer than those of **E** (2.0111 Å) and **F** (2.0171 Å), which is similar to the tendency observed in models **A**−**C** in Table 6. However, the difference between **D** and **E** (0.0164 Å) is smaller than that between **A** and **B** (0.0279 Å). When comparing **D** and **A**, the replacement of the carboxylate ligand with water clearly shortened the Mg−O2 bond by 0.0339 Å, which is consistent with the observation from the crystal structures. With regard to

dx.doi.org/10.1021/ic400671v | *Inorg. Chem.* 2013, 52, 10812−10824

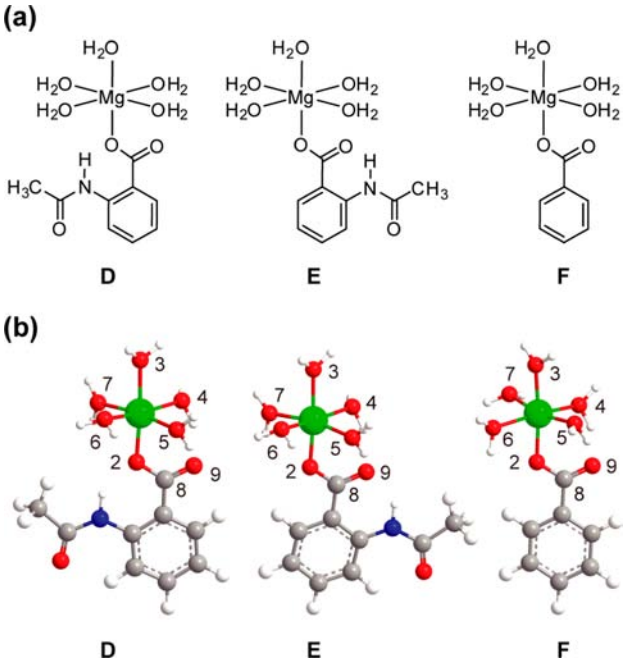

Figure 8. (a) Schematic drawing of initial models **D**–**F** for the DFT calculations. (b) Optimized structures of models **D**–**F**.

the Mg–O (water) bonds of **D**, shortening of the Mg–O bond at the *trans* position could not be found. The mean Mg–O (water) distances did not show significant difference among models **D**—**F**. The small differences of Mg–O2 and Mg–O (water) among these model compounds suggest that the effect of the hydrogen bonds is vague or weakened in the diffused electronic density over the hydrated cation, $[Mg(H_2O)_5]^{2+}$ (i.e., a soft Lewis acid).

The successful coordination with double NH···O hydrogen bonds of the weakly basic carboxylate ligand in **7** strongly suggests the importance of the *cis* configuration. In order to confirm the contribution of the NH···O hydrogen bonds, *cis* configuration, and coordination of water, geometrical optimizations were performed using simplified models. For DFT calculations, a singly hydrogen-bonded ligand was used to separate confused factors. The coordinates of **7** were used as a model after some modifications such as the replacement of methanol by water and the partial deletion of amide groups. Four models were used: one with two NH···O hydrogen bonds to the coordinated O atom (**G**), another with two NH···O bonds to the other uncoordinated O atom (**H**), one without NH···O bonds (**I**), and finally, an unsymmetrical structure with the two types of NH···O (**J**) (see Figure 9). The obtained geometric and electrostatic parameters are summarized in Table S7 in the Supporting Information. In each of the models **G**—**J**, the Mg–O4 and Mg–O5 bonds, at the positions *trans* to the carboxylate, are longer than the other bonds (Mg–O6, Mg–O7). This common tendency is likely because of the *trans* influence, which is attributed to the contribution of charge transfer or delocalization of electrons from the filled orbital on O to the vacant one on Mg. The interaction is not necessarily covalent, as found in soft base–soft acid coordination in transition-metal complexes, and is closely related to the NBO described above. The interactions in the Mg–O bond using hybridization of sphere s and orthogonal p orbitals cause competitive donation to Mg^{2+} along the linear O–Mg–O bond. The anionic carboxylate ion increases the electron

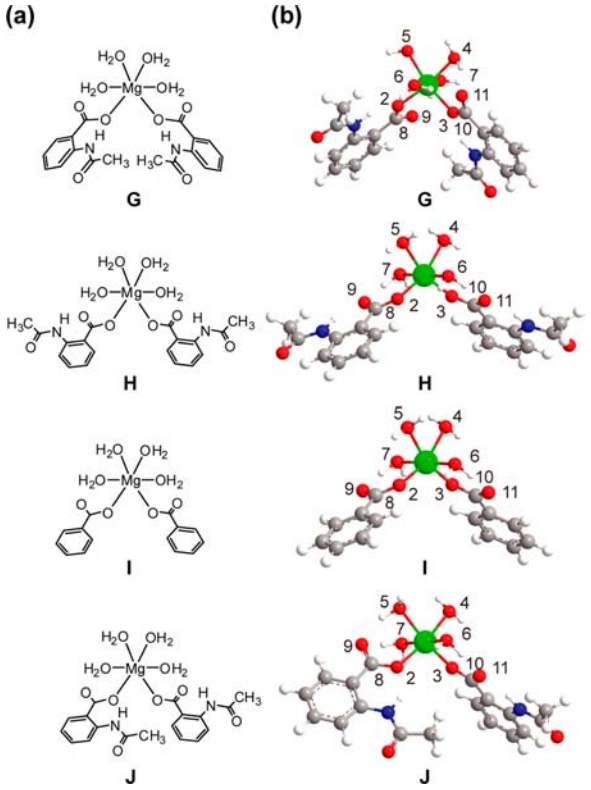

Figure 9. (a) Schematic drawings of initial models **G**–**J** for the DFT calculations. (b) Optimized structures of models **G**–**J**.

density on Mg^{2+}, thereby decreasing acceptable electrons from water. This behavior resembles the *trans* influence found in a covalent metal–sulfur bond.[23] Obvious elongation of the Mg–O2 (carboxylate) bond and shortening of the Mg–O4 (water, *trans*) bond were found in models **G** and **J**, when compared to models **H** and **I**, although the Mg–O5 bond in **G** is long. Interestingly, the unsymmetrical NH···O hydrogen bonds provide uneven Mg–O (carboxylate) bonds with considerable disparity (0.0472 Å), and a short Mg–O5 distance (2.1487 Å) *trans* to a short Mg–O3 (2.0314 Å) was found, in addition to a short Mg–O4 (2.1550 Å) *trans* to a long Mg–O2 (2.0786 Å). The mean Mg–O (water) distance of **J** (2.1389 Å) is smaller than the others (2.1470—2.1482 Å) and longer than those of models **D**—**F** (2.1205—2.1220 Å) with one carboxylate ligand. The relatively small natural charge on Mg in **J** (1.43023) indicates the total electron acceptance from the coordinated O atoms, which is consistent with the shortening of Mg–O bonds. For the other parameters, the tendency is similar to the difference between **A** and **B** in Table 6. The direct NH···O hydrogen bonding to the coordinated O atom results in a small Mo–O–C angle. The hydrogen bond to a carbonyl group shows a relatively large bond order and results in a resonance structure of the carboxylate moiety.

Consequently, coordination of the carboxylate elongates or weakens the Mg–O (water) bond at the *trans* position through electron donation from the anionic oxygen of the carboxylate ligand. The hydrogen bond interacts with an anionic oxygen atom and decreases the negative charge on O by direct NH···O^- interaction or via the conjugated carboxylate anion such as NH···O=C–O^-, which strengthens the Mg–O (water) bond. The strength of the Mg–O (water) bond directly influences the acidity of the water molecule. These results suggest a possible mechanism to control the pK_a of coordinated water via an

dx.doi.org/10.1021/ic400671v | *Inorg. Chem.* 2013, 52, 10812–10824

NH···O hydrogen bond and are described in the following section. In the real protein, an intermolecular hydrogen bond including the coordinated water possibly contributes to the reactivity of the hydrolysis,[10,11] although our isolated model system did not take the possibility into account.

Biological Relevances of NH···O Hydrogen Bonds to the Endonuclease Active Site. The contribution of a carboxylate ion to the acidity of the coordinated water in a magnesium complex has been described in a report by Glusker et al.[14] According to the calculation shown in the report, the replacement of one H_2O molecule of $[Mg(H_2O)_6]^{2+}$ by a carboxylate anion increases the energy of deprotonation by ~80 kcal/mol. The observed elongation of the mean Mg−O (water) distance by increasing the number of carboxylate ligands is consistent with the literature, suggesting the decrease of the acidity. The report also demonstrated that the most acidic water in a $[Mg(H_2O)_5(carboxylate)]^+$ ion is in the position *trans* to the carboxylate ligand although the coordinated water is less acidic than that in $[Mg(H_2O)_6]^{2+}$. By combining the results of the Glusker et al. report and our present work, a new mechanism is proposed for the active site of endonuclease (see Figure 10). A schematic drawing of the magnesium-binding site

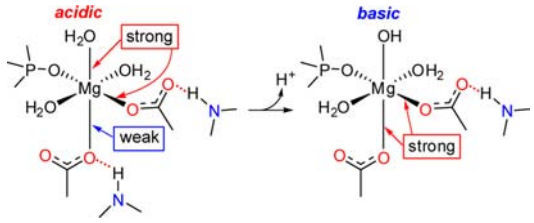

Figure 10. Proposed regulation mechanism of the acidity of the coordinated water; acidic water induced by the NH···O hydrogen-bonded carboxylate ligand (left) and hypothetical basic active site after deprotonation (right), where the hydrogen bond is broken.

in endonuclease *Eco*RV is shown in Figure S2a in the Supporting Information.[5] In the magnesium site of endonuclease, the *cis*-carboxylate configuration is frequently found, where a phosphodiester or phosphate (product) is bound to the Mg ion at the position *trans* to the carboxylate ligand, as shown in Figures 1 and 10, as well as in Figure S2a in the Supporting Information. The carboxylate ligand forms an NH···O=C hydrogen bond with the NH on the peptide backbone, which probably stabilizes the tight binding of the substrate, i.e., Mg−O−P bond. The carboxylate forming the NH···O hydrogen bond weakly coordinates to Mg, strengthening the Mg−O (water) bond in the *trans* position, thus increasing the acidity of water (see Figure 10). The direct NH···O hydrogen bond to the coordinated O is the most effective in increasing the acidity of water. If the ligand forms double NH···O hydrogen bonds, it is the best. Deprotonation of the acidic water molecule gives the relatively weak conjugate base, Mg−OH, according to the fundamental acid−base chemistry. If the hydrogen bond is cleaved simultaneously or subsequently, the basicity of the hydroxide group must increase dramatically (see Figure 10). The basic OH group can deprotonate the neighboring outer-sphere water and produce an external hydroxide, which then attacks the phosphodiester linkage of the adjacent substrate. The present switching mechanism (i.e., the formation and cleavage of NH···O hydrogen bond) is possible in some proteins. Figure S2b in the Supporting Information shows an endonuclease active site found in an avian influenza polymerase.[3] The imidazole nitrogen is located close to the carboxylate ligand, suggesting the presence of a potential (imidazole)NH···O hydrogen bond (N···O = 3.22, 3.82 Å), although NH is illustrated in the opposite direction. Rotation and/or tautomerism of the imidazole group could act as a switch. In magnesium-containing proteins, dinuclear or trinuclear catalytic sites were found where the Mg ion plays the role of a binding site for the substrate and/or a reactive site.[5,7,61] The μ-carboxylate bridged Mg−OCO−Mg structure resembles the NH···OCO−Mg hydrogen bond. Our results suggest that the Mg ion, or Lewis acid, acts like the NH group in a hydrogen bond. Therefore, the concentration of the Mg^{2+} ion influences the catalytic activity as well as construction of the binding site.[7] In the mechanism of phosphatase activity, direct attack of the Mg-binding carboxylate anion (Asp residue) to the phosphate ester has also been proposed.[39,62,63] The reaction must be strictly dependent on the basicity of the carbonyl group of Asp residue, with the hydrogen bond also contributing significantly.

CONCLUSIONS

The magnesium−carboxylate complexes containing intramolecular NH···O hydrogen bonds revealed significant contributions to the bond character of the Mg−O linkage (Figure 11). Direct NH···O hydrogen bonding to the

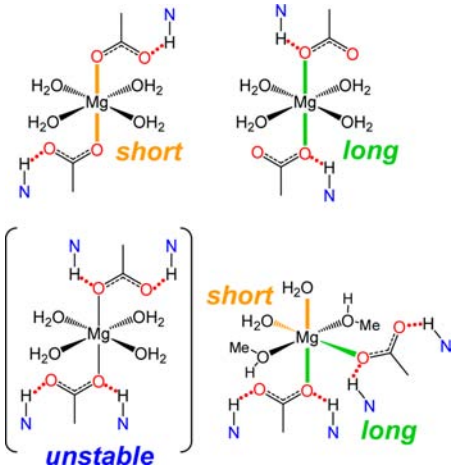

Figure 11. Contributions of the intramolecular NH···O hydrogen bonds to Mg−O bonds.

coordinated oxygen atom elongates the Mg−O bond while a hydrogen bond to the carbonyl group shortens the Mg−O bond. Doubly NH···O hydrogen-bonded carboxylate is a Lewis base that is too soft or weak; therefore, it cannot coordinate to the Mg ion in a *trans* configuration; however, it was successful in *cis*-dicarboxylate coordination. The significantly weak Mg−O (carboxylate) bond strengthens the Mg−O (water) bond, similar to the *trans* influence caused by a competitive charge-transfer or delocalization of electrons. The experimental and theoretical results led to the proposed switching mechanism for controlling the acidity of the coordinated water and basicity of the deprotonated Mg−OH moiety. Our switching mechanism presents a possible solution to the problem of incompatible properties such as a strong acid with a strong conjugate base of the coordinated water required for catalytic activity in hydrolysis.

■ ASSOCIATED CONTENT

Supporting Information

X-ray crystallographic data for models **1**−**8**, and 2,6-$(CH_3CONH)_2C_6H_3COOH$ in CIF format, details for the ligand (Table S1, Figure S1), geometrical parameters of models **3**−**6** (Tables S2−S5), results of DFT calculations (Tables S6, S7), schematic drawing of the active sites (Figure S2). This material is available free of charge via the Internet at http://pubs.acs.org.

■ AUTHOR INFORMATION

Corresponding Author

*E-mail: tokamura@chem.sci.osaka-u.ac.jp.

Notes

The authors declare no competing financial interest.

■ ACKNOWLEDGMENTS

This work was supported by JSPS KAKENHI (Grant No. 23655049).

■ REFERENCES

(1) Sigel, H.; Sigel, A., Eds. *Compendium on magnesium and its role in biology, nutrition and physiology*; Marcel Dekker: New York, 1990; Vol. *26*.
(2) Goldgur, Y.; Dyna, F.; Hickman, A. B.; Jenkins, T. M.; Graigie, R. *Proc. Natl. Acad. Sci. U.S.A.* **1998**, *95*, 9150−9154.
(3) Yuari, P.; Bartlam, M.; Lou, Z.; Chen, S.; Zhou, J.; He, X.; Lv, Z.; Ge, R.; Li, X.; Deng, T.; Fodor, E.; Rao, Z.; Liu, Y. *Nature* **2009**, *458*, 909−913.
(4) Lebbink, J. H. G.; Fish, A.; Reumer, A.; Natrajan, G.; Winterwerp, H. H. K.; Sixma, T. K. *J. Biol. Chem.* **2010**, *285*, 13131−13141.
(5) Kostrewa, D.; Winkler, F. K. *Biochemistry* **1995**, *34*, 683−696.
(6) Bujacz, G.; Jaskólski, M.; Alexandratos, J.; Wlodawer, A.; Merkel, G.; Katz, R. A.; Skalka, A. M. *Structure* **1996**, *4*, 89−96.
(7) Ho, M.-H.; VIvo, M. D.; Peraro, M. D.; Klein, M. L. *J. Am. Chem. Soc.* **2010**, *132*, 13702−13712.
(8) Black, C. B.; Huang, H.-W.; Cowan, J. A. *Coord. Chem. Rev.* **1994**, *135/136*, 165−202.
(9) Cowan, J. A. *Chem. Rev.* **1998**, *98*, 1067−1087.
(10) Cowan, J. A. *BioMetals* **2002**, *15*, 225−235.
(11) Black, C. B.; Cowan, J. A. *J. Am. Chem. Soc.* **1994**, *116*, 1174−1178.
(12) Lesnichin, S. B.; Shenderovich, I. G.; Muljati, T.; Silverman, D.; Limbach, H.-H. *J. Am. Chem. Soc.* **2011**, *133*, 11331−11338.
(13) López-Canut, V.; Ruiz-Pernía, J. J.; Castillo, R.; Moliner, V.; Tuñón, I. *Chem.—Eur. J.* **2012**, *18*, 9612−9621.
(14) Katz, A. K.; Glusker, J. P.; Markham, G. D.; Bock, C. W. *J. Phys. Chem. B* **1998**, *102*, 6342−6350.
(15) Fothergill, M.; Goodman, M. F.; Petruska, J.; Warshel, A. *J. Am. Chem. Soc.* **1995**, *117*, 11619−11627.
(16) Black, C. B.; Cowan, J. A. *Eur. J. Biochem.* **1997**, *243*, 684−689.
(17) Florián, J.; Åqvist, J.; Warshel, A. *J. Am. Chem. Soc.* **1998**, *120*, 11524−11525.
(18) Klähn, M.; Rosta, E.; Warshel, A. *J. Am. Chem. Soc.* **2006**, *128*, 15310−15323.
(19) Okamura, T.; Yamamoto, H.; Ueyama, N. In *Hydrogen Bonding and Transfer in the Excited State*; Han, K.-L., Zhao, G.-J., Eds.; John Wiley & Sons Ltd: Chichester, U.K., 2011; Vol. 2, pp 609−626.
(20) Ueyama, N.; Okamura, T.; Nakamura, A. *J. Am. Chem. Soc.* **1992**, *114*, 8129−8137.
(21) Ueyama, N.; Okamura, T.; Nakamura, A. *J. Chem. Soc., Chem. Commun.* **1992**, 1019−1020.
(22) Adman, N.; Watenpaugh, K. D.; Jensen, L. H. *Proc. Natl. Acad. Sci. U. S. A.* **1975**, *72*, 4854−4858.
(23) Okamura, T.; Tatsumi, M.; Omi, Y.; Yamamoto, H.; Onitsuka, K. *Inorg. Chem.* **2012**, *51*, 11688−11697.
(24) Okamura, T.; Ushijima, Y.; Omi, Y.; Onitsuka, K. *Inorg. Chem.* **2013**, *52*, 381−394.
(25) Okamura, T.; Kunisue, K.; Omi, Y.; Onitsuka, K. *Dalton Trans.* **2013**, *42*, 7569−7578.
(26) Okamura, T.; Taniuchi, K.; Lee, K.; Yamamoto, H.; Ueyama, N.; Nakamura, A. *Inorg. Chem.* **2006**, *45*, 9374−9380.
(27) Onoda, A.; Yamada, Y.; Nakayama, Y.; Takahashi, K.; Adachi, H.; Okamura, T.; Nakamura, A.; Yamamoto, H.; Ueyama, N.; Vyprachticky, D.; Okamoto, Y. *Inorg. Chem.* **2004**, *43*, 4447−4455.
(28) Onoda, A.; Yamada, Y.; Okamura, T.; Yamamoto, H.; Ueyama, N. *Inorg. Chem.* **2002**, *41*, 6038−6047.
(29) Drake, S. R.; Sanderson, K. D.; Hursthouse, M. B.; Malik, K. M. A. *Inorg. Chem.* **1993**, *1993*, 1041−1044.
(30) Yamada, Y.; Ueyama, N.; Okamura, T.; Mori, W.; Nakamura, A. *Inorg. Chim. Acta* **1998**, *275*−*276*, 43−51.
(31) Onoda, A.; Yamada, Y.; Takeda, J.; Nakayama, Y.; Okamura, T.; Doi, M.; Yamamoto, H.; Ueyama, N. *Bull. Chem. Soc. Jpn.* **2004**, *77*, 321−329.
(32) Altomare, A.; Burla, M. C.; Camalli, M.; Cascarano, M.; Giacovazzo, C.; Guagliardi, A.; Polidori, G. *J. Appl. Crystallogr.* **1994**, *27*, 435.
(33) Sheldrick, G. M. *Acta Crystallogr., Sect. A: Found. Crystallogr.* **2008**, *A64*, 112−122.
(34) Frisch, M. J.; Trucks, G. W.; Schlegel, H. B.; Scuseria, G. E.; Robb, M. A.; Cheeseman, J. R.; Montgomery, J. A., Jr.; Vreven, T.; Kudin, K. N.; Burant, J. C.; Millam, J. M.; Iyengar, S. S.; Tomasi, J.; Barone, V.; Mennucci, B.; Cossi, M.; Scalmani, G.; Rega, N.; Petersson, G. A.; Nakatsuji, H.; Hada, M.; Ehara, M.; Toyota, K.; Fukuda, R.; Hasegawa, J.; Ishida, M.; Nakajima, T.; Honda, Y.; Kitao, O.; Nakai, H.; Klene, M.; Li, X.; Knox, J. E.; Hratchian, H. P.; Cross, J. B.; Adamo, C.; Jaramillo, J.; Gomperts, R.; Stratmann, R. E.; Yazyev, O.; Austin, A. J.; Cammi, R.; Pomelli, C.; Ochterski, J. W.; Ayala, P. Y.; Morokuma, K.; Voth, G. A.; Salvador, P.; Dannenberg, J. J.; Zakrzewski, V. G.; Dapprich, S.; Daniels, A. D.; Strain, M. C.; Farkas, O.; Malick, D. K.; Rabuck, A. D.; Raghavachari, K.; Foresman, J. B.; Ortiz, J. V.; Cui, Q.; Baboul, A. G.; Clifford, S.; Cioslowski, J.; Stefanov, B. B.; Liu, G.; Liashenko, A.; Piskorz, P.; Komaromi, I.; Martin, R. L.; Fox, D. J.; Keith, T.; Al-Laham, M. A.; Peng, C. Y. ; Nanayakkara, A.; Challacombe, M.; Gill, P. M. W.; Johnson, B.; Chen, W.; Wong, M. W.; Gonzalez, C.; Pople, J. A. *Gaussian 03 (Revision E.01)*; Gaussian, Inc.: Pittsburgh PA, 2004.
(35) Irish, D. E.; Semmler, J.; Taylor, N. J.; Toogood, G. E. *Acta Crystallogr., Sect. C: Cryst. Struct. Commun.* **1991**, *47*, 2322−2324.
(36) Dey, B. K.; Karmakar, A.; Baruash, J. B. *J. Mol. Catal. A: Chem.* **2009**, *303*, 137−140.
(37) Carrell, C. J.; Carrell, H. L.; Erlebacher, J.; Glusker, J. P. *J. Am. Chem. Soc.* **1988**, *110*, 8651−8656.
(38) Chan, S.; Segelke, B.; Lekin, T.; Krupka, H.; Cho, U. S.; Kim, M.-y.; So, M.; Kim, C.-Y.; Naranjo, C. M.; Rogers, Y. C.; Park, M. s.; Waldo, G. S.; Pashkov, I.; Cascio, D.; Perry, J. L.; Sawaya, M. R. *J. Mol. Biol.* **2004**, *341*, 503−517.
(39) Gomez, G. A.; Morisseau, C.; Hammock, B. D.; Christianson, D. W. *Biochemistry* **2004**, *43*, 4716−4723.
(40) Babu, C. S.; Dudev, T.; Lim, C. *J. Am. Chem. Soc.* **2013**, *135*, 6541−6548.
(41) Babu, C. S.; Lim, C. *J. Am. Chem. Soc.* **2010**, *132*, 6290−6291.
(42) Dudev, T.; Lim, C. *J. Am. Chem. Soc.* **2006**, *128*, 1553−1561.
(43) Dudev, T.; Lim, C. *Acc. Chem. Res.* **2007**, *40*, 85−93.
(44) Dudev, T.; Lim, C. *Annu. Rev. Biophys.* **2008**, *37*, 97−116.
(45) Izumi, M.; Ichikawa, K.; Suzuki, M.; Tanaka, I.; Rudzinski, K. W. *Inorg. Chem.* **1995**, *34*, 5388−5389.
(46) Rao, C. P.; Rao, A. M.; Rao, C. N. R. *Inorg. Chem.* **1984**, *23*, 2080−2085.
(47) Lewinski, K.; Lebioda, L. *J. Am. Chem. Soc.* **1986**, *108*, 3693−3696.
(48) Gao, S.; Huo, L.-H.; Zhang, Z.-Y.; Kong, L.-L.; Zhao, J.-G. *Acta Crystallogr., Sect. E: Struct. Rep. Online* **2004**, *60*, m679−m681.
(49) Senkovska, I.; Kaskel, S. *Eur. J. Inorg. Chem.* **2006**, 4564−4569.

(50) Julian, M. O.; Day, V. W.; Hoard, J. L. *Inorg. Chem.* **1973**, *12*, 1754−1757.
(51) Arlin, J.-B.; Florence, A. J.; Johnston, A.; Kennedy, A. R.; Miller, G. J.; Patterson, K. *Cryst. Growth Des.* **2011**, *11*, 1318−1327.
(52) Curry, M. E.; Eggleston, D. S.; Hodgson, D. J. *J. Am. Chem. Soc.* **1985**, *107*, 8234−8238.
(53) Havere, W. v.; Lenstra, A. T. H. *Acta Crystallogr., Sect. B: Struct. Crystallogr. Cryst. Chem.* **1980**, *36*, 2414−2416.
(54) Karipides, A. *Inorg. Chem.* **1979**, *18*, 3034−3037.
(55) Duan, X.; Lin, J.; Li, Y.; Zhu, C.; Meng, Q. *CrystEngComm* **2008**, *10*, 207−216.
(56) Liu, H.-K.; Tsao, T.-H.; Zhang, Y.-T.; Lin, C.-H. *CrystEngComm* **2009**, *11*, 1462−1468.
(57) Tang, Y.-Z.; Tan, Y.-H.; Chen, S.-H.; Chao, Y.-W.; Wang, P. *J. Coord. Chem.* **2008**, *61*, 1244−1252.
(58) Weinhold, F.; Landis, C. R. *Valency and Bonding. A Natural Bond Orbital Donor-Acceptor Perspective*; Cambridge University Press: Cambridge, U.K., 2005.
(59) Weinhold, F.; Landis, C. R. *Discovering Chemistry with Natural Bond Orbitals*; John Wiley & Sons, Inc.: Hoboken, NJ, 2012.
(60) Pearson, R. G. *J. Am. Chem. Soc.* **1963**, *85*, 3533−3539.
(61) Steitz, T. A.; Steitz, J. A. *Proc. Natl. Acad. Sci. U.S.A.* **1993**, *90*, 6498−6502.
(62) Morais, M. C.; Zhang, W.; Baket, A. S.; Zhang, G.; Dunnaway-Mariano, D.; Allen, K. N. *Biochemistry* **2000**, *39*, 10385−10396.
(63) Vivo, M. D.; Ensing, B.; Klein, M. L. *J. Am. Chem. Soc.* **2005**, *127*, 11226−11227.